12th IEA Heat Pump Conference 2017

ORC Driven Heat Pump Running on Gas Bearings for Domestic Applications: Proof of Concept and Thermo-Economic Improvement Potential

Violette Mounier[a,*], Jürg Schiffmann[a]

[a] Laboratory for Applied Mechanical Design, Ecole Polytechnique Fédérale de Lausanne, EPFL
Rue de la Maladière 71b, Neuchâtel, 2000, Switzerland

Abstract

ORC driven Heat Pumps (HP-ORC) offer a promising technology of thermally driven heat pumps (TDHPs) for domestic applications. Recently, a 40 kW HP-ORC unit based on gas supported turbomachinery has been investigated in which the ORC radial turbine drives the HP centrifugal compressor, offering an oil free and high power density solution. The radial compressor and the radial turbine have tip diameters of the order of 20 mm and the system has been tested at rotor speeds in excess of 200 krpm with shaft powers up to 2.4 kW, running with R134a. The compressor and the turbine were operated at pressure ratios of up to 2.8 and 4.4, while reaching thermal COP of the order of 1.5 and isentropic compressor and turbine efficiencies in excess of 70%, thus validating the HP-ORC concept based on small-scale turbomachinery. However, performance limitations were encountered due to suboptimal heat exchanger, working fluid and turbomachinery design. This article presents a full thermo-economic optimization of the HP-ORC enabling the identification of the best trade-off Investment Cost/ COP. Several working fluids have then been compared, revealing that a compromise is to be found between best cost/efficiency trade-off, highest performances achievable and technical feasibility. It also showed a thermal COP improvement potential up to 30% compared to the existing experimental system. Finally, the thermo-economic results of the HP-ORC have been compared with other typical TDHPs, such as absorption heat pump.

© 2017 Stichting HPC 2017.
Selection and/or peer-review under responsibility of the organizers of the 12th IEA Heat Pump Conference 2017.

Keywords : Thermally driven Heat Pumps; Organic Rankine Cycle; Absorption Heat Pumps; ORC driven Heat Pump, Small Scale Turbomachinery; Gas Bearings; Multi-Objective Optimization;Thermo-economic, Evolutionary Algorithm

1. Introduction

Thermally driven heat pumps (TDHPs) systems are promising technologies to provide more environmentally friendly domestic heating, especially when renewable primary heat sources are used such as waste heat, solar, or biomass. For that reason, gas engine driven heat pumps (GEHPs), which are solely powered by liquid or gas fossil fuels, have been eluded from the present study. The predominant remaining technology in the literature and on the market are sorption systems, and more especially absorption heat pumps. However, due to the recent developments of small scale and oil free turbomachinery [1,2], the Organic Rankine Cycle driven heat pumps (HP-ORC) are reconsidered. HP-ORC are composed of a bottoming vapor compression Heat Pump (HP) cycle and of a topping Organic Rankine Cycle (ORC) in which the ORC turbine directly drives the HP compressor. Different concepts of HP-ORC for heating or cooling application are proposed in the literature, where the HP and the ORC cycles are either mechanically [3,4] or electrically coupled [5,6]. Electrically coupled systems offer more flexibility, but lead to higher investment costs due to the addition of power conversion units. Therefore, directly mechanically coupled

HP-ORCs are considered in this study. In the lower power range (5-50 kW), both HP and ORC concepts predominantly use volumetric expansion and compression devices [7]. Nevertheless, recent studies performed by Demierre et al. [8] and Schiffmann et al.[9,10], suggests that the operation of dynamic machines along with the use of gas-lubricated bearings is a promising as it offers an oil free solution for low capacity heat pumps. Demierre et al. [8,11] designed and operated a HP-ORC system, based on gas supported high speed radial turbo machinery for heating capacity of 40 kW achieving a measured COP of 1.5. Moreover, as highlighted by Mounier at al. [12], the HP-ORC system running on gas bearings is highly competitive with typical absorption heat pumps regarding performance and operating range [12]. The thermo-economic comparison is yet missing. Moreover, only R-134a fluid has been studied for the HP-ORC in [12], and it is likely that other working fluids could perform better. Finally, HP-ORC performance limitations were revealed during the test-phase, highlighting suboptimal turbomachinery, shaft, and heat exchanger design. Therefore, the goal of the investigation is to assess the potential of HP-ORC running on gas bearings, towards a performance/operating range/economic comparison with typical Single Effect Absorption Heat Pump (SEAbs).
The objectives are to: (1) build thorough thermodynamic and economic models of the HP-ORC and the SEAbs system, (2) compare the TDHPs on different operating conditions (3) perform a thermo-economic comparison of the TDHPs using a multi objective optimization (4), identify and analyse key thermodynamic and/or turbomachinery parameters of the HP-ORC and (5) check the potential of improvement of the current HP-ORC prototype. For this purpose, a steady state thermodynamic model of the HP-ORC and SEAbs is proposed, as well as an economic model for every component of both systems. The results suggest that the two TDHPs are highly competitive, regarding their performances with different operating ranges, and their thermo-economic trade-offs. When optimizing both the COP and the investment cost for the HP-ORC, the results show that a compromise is to find between the R-134a and the R-152a working fluid depending on the trade-off target, and that there is a COP improvement potential of 30 % to be reached on the experimental level.

2. Systems description and modelling

The thermodynamic model is based on a typical water-brine heat pump system for floor heating of a small multi dwelling building. The hot source is a thermal oil heated by a boiler whose temperatures are taken from typical low grade power ORCs [13] and absorption heat pumps [14]. Brine temperatures at the condensers and evaporators are set according to the EHPA standards [15]. The thermal properties of the brines and thermal oil have been computed with CoolProp [16]. To evaluate the performance of the HP-ORC, the Coefficient of Performance (COP) is computed as followed:

$$COP = \frac{Q_{sink}}{Q_{hot} + \frac{W_p}{0.56}} \quad (1)$$

Where Q_{sink} is the energy output delivered at the heat sink, Q_{hot} the energy input at the hot source to drive the cycles, and W_p the pump power. In order to compare system performances strictly based on conversion of fuel into heat, the pump power is divided by 0.56, to take into account for electric grid losses and for the efficiency of a modern gas-fired combined cycle power plant. The operating conditions of the model are summarized in Table 1.

Table 1 : Operating conditions of the HP-ORC and of the SEAbs

Nomenclature	Term	Unit	Value
Qsink	Heat power output	kW	40
ηis,pump	Pump isentropic efficiency	%	60
DTsc,pump	Subcooling before ORC pump	K	7
DTmin,regHX	Pinch in the regenerative heat exchangers (ORC regenerator, SEAbs Solution Heat Exchanger, SEAbs precooler)	K	10
Tsink,in	Sink Inlet Temperature	°C	[30, 47]
Tsink,out	Sink outlet Temperature	°C	[35, 55]
Thot,in	Hot Source Inlet Temperature	°C	[120,150,180,210]
Thot,out	Hot Source outlet Temperature	°C	80
Tchill,in	Cold Source Inlet Temperature	°C	[-7, 7]
Tchill,out	Cold Source outlet Temperature	°C	[-4, 4]

2.1 ORC driven Heat Pumps running on gas bearings

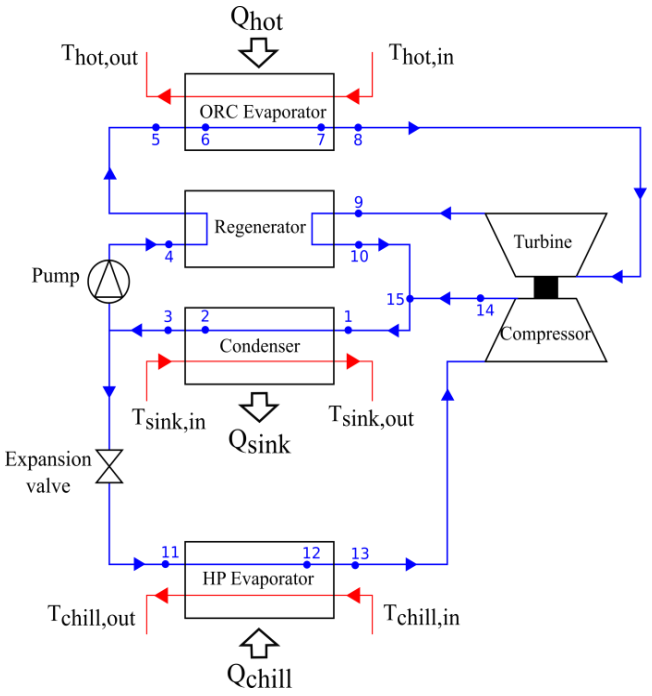


Figure 1 : Schematic of the HP-ORC cycle

The cycle in Figure 1 is composed of a topping Organic Rankine Cycle and of a bottoming vapor compression Heat Pump cycle. The topping cycle is composed of a pump, an ORC evaporator, a turbine, a regenerator and a condenser. The turbine drives the compressor of the bottoming cycle, composed of an HP evaporator, a compressor, a condenser and an expansion valve. The two vapor streams leaving the compressor and the turbine are adiabatically mixed in (15). In cases where the regenerator is not needed, states 4 and 5 (resp. 9 and 10) are equivalent. Q_{hot} is the thermal power delivered from the system hot source to the ORC evaporator, Q_{chill} is the thermal power delivered by the cold source to the HP evaporator and Q_{sink} is the thermal power recovered from the condenser. A Compressor Turbine Unit (CTU) is implemented to fulfil both the expansion and the compression of the two loops, where the ORC radial inflow turbine directly drives the HP centrifugal compressor. Both turbomachineries are coupled on the same gas bearing supported rotor. The gas bearings (journal and thrust bearings) are of dynamic type and are lubricated with vapor phase refrigerant fluid, ensuring oil free operation. The HP-ORC simulation procedure consists of two iteration layers in order to identify first the cycle saturation temperatures and secondly the CTU operating properties. The calculation is initialized with a best guess of the rotor speed N_{rot}, turbine and compressor isentropic efficiencies ($\eta$is,t $\eta$is,c) as well as with an initial set of saturated temperatures. The two iterations operate successively using a nonlinear solver, until power and mass balances along the components and targeted pinches in the heat exchangers are satisfied. The thermophysical and transport properties of the HP-ORC working fluids are computed using REFPROP 9.1 [17]. The CTU modelling is performed based on similarity concepts developed by Balje [12,18], with a penalty factor of 0.9 for radial turbines in order to account for reduced scale turbomachinery issues such as reduced Reynolds number, increased relative surface roughness and tip clearance. The CTU power balance includes the mechanical losses resulting from the bearings and the rotor [8], whose geometry is scaled with rotor speed. Finally, the simulation is subjected to a set of constraints. The heat exchanger pinches are first limited such as the pressure ratios in both the turbine and compressor are realistic. The maximum pressure ratio of the turbine is limited to 8 considering a single stage radial turbine with convergent nozzle, while the maximum pressure ratio in a single stage compressor is set to 5. If the compressor pressure ratio exceeds 5, the simulation implements a second stage. A maximum ORC evaporation pressure of 70 bar is set as a limit. Finally, the simulation constrains both the compressor and the turbine to not operate under the saturation line as it may lead to bearing failure and premature blade erosion at high rotor speeds. The working fluid selection for the HP-ORC remains an open question, as it needs to perform well in the two thermal loops which are subjected to different pressure levels. Therefore, R-134a, R-152a (HP applications) and R-245fa (ORC applications) are considered in the study. Note that the replacements fluids of R-134a and R-245fa (resp. R-1234yf/R-1234ze and R-1233zd) are not included although their GWP is low, as the goal is test refrigerants with different thermodynamic behaviours. All the selected refrigerants are non-flammable, in order to ensure safe operation for domestic applications.

2.2 Single Effect Absorption Heat Pump

Absorption Heat Pumps (AHPs) are characterized by their number of effects or stages, as well by their refrigerant/absorbent pair. The most common and simple configurations are Single Effect Absorption Heat Pumps (SEAbs) working with $LiBr/H_2O$ or NH_3/H_2O. However, the operating range of AHPs working with $LiBr/H_2O$ for heating applications is limited by crystallization and freezing issues [19]. The number of stages or effects can be increased to enhance the COP of the AHPs, at the penalty, however, of an increasing number of heat exchangers. Therefore, in order to have a fair comparison with HP-ORC regarding the number of heat exchanger units, only the Single Effect Absorption heat pump (SEAbs) working with NH_3/H_2O have been considered, showed in Figure 2. The implemented SEAbs model is based and adapted from Herold et al. [20]. The thermophysical properties of the Ammonia-Water mixtures are obtained with an adapted model from Tillner Roth et al. integrated in REFPROP 9.1[17,21]. The transport properties models of Conde [22] and of Wilke [23] are used for liquid and vapor phases respectively. The cycle is first calculated with initial set of mass flows, the saturation temperatures in the SEAbs condenser, absorber (saturated liquid) and SEAbs evaporator with a vapor quality of 0.998. The cycle calculation is iterated until the total and ammonia mass balance over the cycle components, overall energy balance as well as the targeted pinches are satisfied.

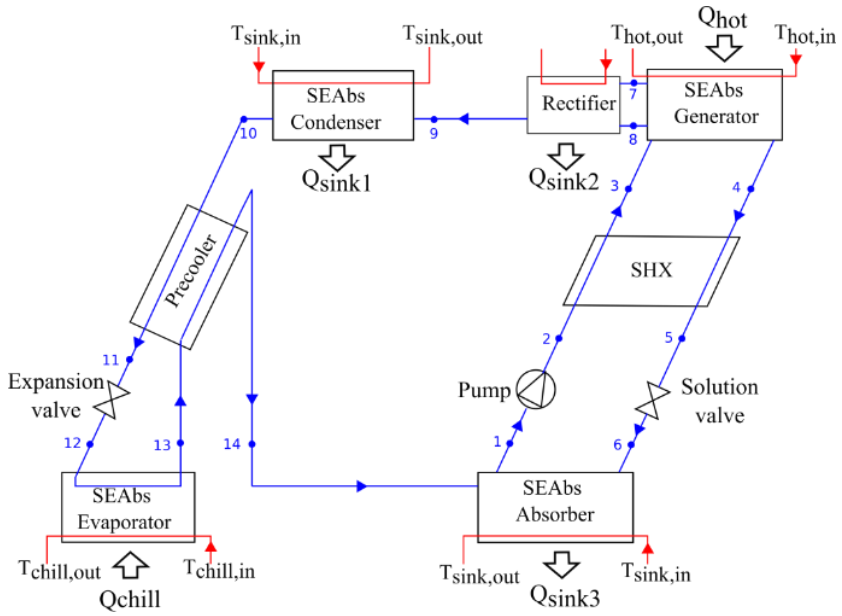


Figure 2 : Schematic of the SEAbs cycle

3. Economic model

The overall investment cost $C_{I,Tot}$ of TDHPs is mostly determined by the following components: the boiler, the Heat Exchangers (HX), the CTU, the pump, the circuit valves and the ground source heat exchanger (GHX). As the boundary conditions of both TDHPs are the same, the cost of the GHX, the boiler and the pump have been assumed equal, and therefore neglected. The heat exchangers considered for both systems are plate heat exchangers (PHE), for their compactness and performance, except for the SEAbs rectifier which is of helical coil type (HC). The cost of the PHEs and HCs are estimated using the correlation and data presented by Henchoz et al. [24], which are based on catalogue prices for CO_2 network Plate Heat Exchangers (PHEs) and Shell and Tubes. Since the HX cost is primarily driven by its area [25], a model based on the Logarithmic Mean Temperature Difference (LMTD) [26] and on the Logarithmic Mean Concentration Difference (LMCD) [27] has been built. Figure 3 shows the schematic of a typical PHE and HC as well as its main dimensions, which have been chosen accordingly with average values found at suppliers. Table 2 summarizes the different empirical correlations used for the evaluation of the heat transfer coefficients accordingly with the flow regimes encountered, respectively when mass transfer process occurs or not. The correlations used for the two-phase regimes have been chosen according to the recommendations made by Amalfi et al [28].

Table 2 : Heat transfer correlations for heat exchange area evaluation for the different encountered flow conditions and processes

Flow condition/Process	Correlation
Single Phase	Martin [29]
Condensing	Yan et al [30]
Evaporating	Danilova et al [31]
Absorption (SEAbs absorber)	Lee et al. [27]
Desorption (SEAbs generator)	Taboas et al [32]
Rectification (Rectifier)	Qasrawi et al. [33]

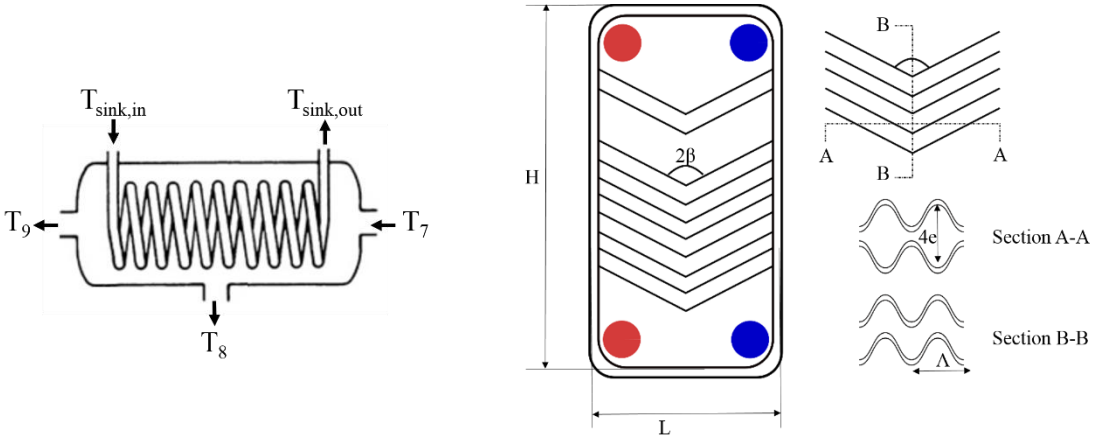


Figure 3 : Schematic and main dimensions of a PHE (left) and of a HC (right)

The cost of the SEAbs's Solution Valve (SV) is set through available product on the market. Concerning the cost of the CTU in the HP-ORC, no correlation exists due to the prototype stage of the technology. Nevertheless, thanks to the experience gathered on the first prototypes, the manufacturers estimate a unitary cost of 500 $, considering series production. Expansion valve, piping and auxiliaries' costs are neglected. Table 3 summarizes the different cost correlations for the aforementioned components.

Table 3: Cost correlations of the different TDHPs components

Cycle	Component	Cost Correlation [$]	Reference
HP-ORC	CTU	$C_{CTU}=500$	Internal investigation
HP-ORC /SEAbs	PHE	$C_{PHE,i}=147+407.A_{PHE,i}^{0.803}$	Henchoz et al. [24]
SEAbs	HC	$C_{HC}=193+1161.A_{HC}^{0.9119}$	Henchoz et al. [24]
SEAbs	SV	$C_{SV}=500$	Market research [34].

The total investment costs respectively for the HP-ORC and the SEAbs are therefore expressed as follows:

$$C_{I,Tot,HP\text{-}ORC}=\sum_{j} C_{PHE,j}+C_{CTU} \quad (2)$$

$$C_{I,Tot,SEAbs}=\sum_{j} C_{PHE,j}+C_{HC}+C_{SV} \quad (3)$$

4. Results and discussion

4.1 Comparison of HP-ORC and SEAbs: effect of operating conditions on performance

Figure 4a 4b shows the evolution of the TDHPs COP in heating mode with the hot source temperature, for two different operating conditions OP1 and OP2, which are summarized in Table 4. OP1 corresponds to a brine-water heat pump whereas OP2 characterizes a typical operation point of an air-water system. The three different working fluids presented above have been tested for the HP-ORC.

Table 4: Boundary conditions of the TDHPs

Parameter	Operating condition Nomenclature	OP1 Value	OP2 Value

Heat sink Inlet Temperature	Tsink,in	30 °C	47 °C
Heat sink Outlet Temperature	Tsink,out	35 °C	55 °C
Cold Source Inlet Temperature	Tchill,in	7 °C	-7 °C
Cold Source outlet Temperature	Tchill,out	4 °C	-4 °C

For this comparison based purely on COP as a function of the hot source temperature and without considering HX size and cost, the pinches (DTmin) in the heat exchangers have been fixed at 10 K for the hot sources (ORC evaporator/SEAbs generator) and 2 K for the cold sources (HP evaporator/SEAbs evaporator) and for the sinks (HP ORC condenser/SEAbs condenser/SEAbs Absorber/SEAbs rectifier). For the HP-ORC, the turbine superheat $DT_{sh,turb}$ has been set to 50 K while the other thermodynamic variables are the same as presented in Table 1. The COP values are lower for OP2 compared to OP1, which is in accordance with thermodynamic principles as the pressure ratios are lower in the turbine and higher across the compressor. For the hot source temperatures below 180°C, it can be seen that the HP-ORC's working fluids yield similar COPs, while above 180°C, higher discrepancies appear. At 180°C, R-134a presents the highest COP, while R-152a and R-245fa come in second and third position. However, at 210°C, R-152a performs better. This is due to the single stage turbine ratio limited to 8, already achieved by R-134a at this point. For OP1, the SEAbs yields a rather constant COP of 1.51. If the SEAbs presents the best COP at 120°C, HP-ORCs perform better at higher hot source temperatures. This is due to the limitation of the desorption/absorption process, which already achieves its maximum potential at 120°C. In OP2, as the absorption and condensation temperatures are higher, increased hot source temperatures tend to increase the COP in contrast to OP1. Above 150°C, the SEAbs offers very similar performances as the HP-ORC, but without outperforming it. The two systems are therefore highly competitive regarding their performance and operating range. Nevertheless, beyond the HP-ORC performance, the turbocompressor design parameters are of great interest. Considering the working fluid R-152a, Table 5 shows the turbocompressor parameters as a function of the different operating conditions and hot source temperatures.

Table 5: R-152a Turbocompressor design parameters.

	Thot,in (°C)	120		150		180		210	
Term	OP	OP1	OP2	OP1	OP2	OP1	OP2	OP1	OP2
Nrot	[krpm]	227	214	290	271	369	331	381	314
dt	[mm]	13	12	12	11	11	10	11	12
dc,stage1	[mm]	21	18	19	16	17	17	18	19
dc,stage2	[mm]	-	25	-	20	-	17	-	18
ηis,t (-)	[-]	0.79	0.73	0.82	0.76	0.81	0.81	0.81	0.81
ηis,c,stage1(-)	[-]	0.84	0.86	0.87	0.87	0.87	0.86	0.86	0.86
ηis,c,stage2(-)	[-]	-	0.67	-	0.77	-	0.84	-	0.85

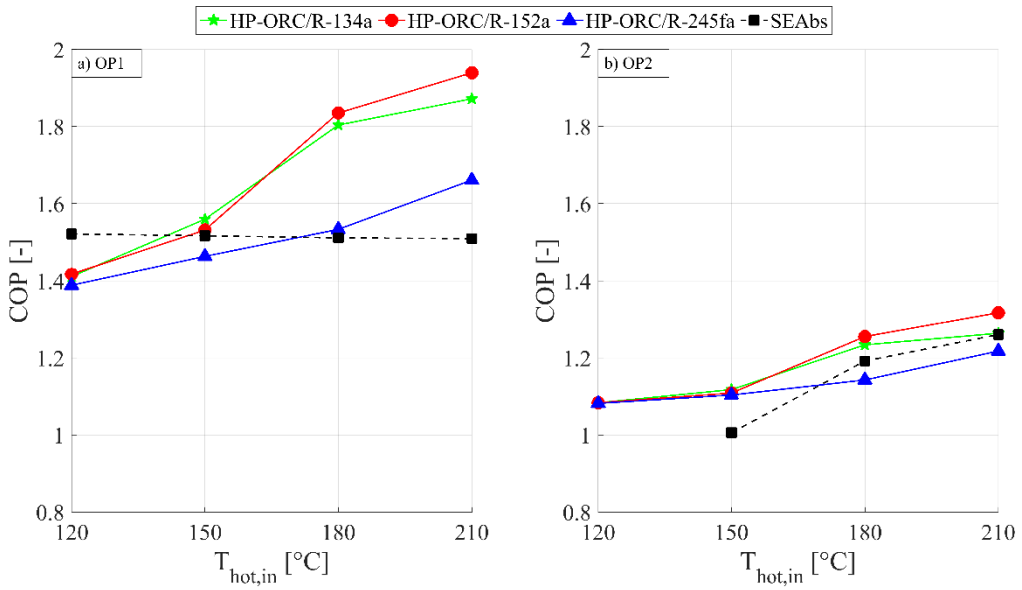


Figure 4 : COP versus the hot source temperature for two operating conditions (OP1 &OP2) and TDHPs cycles (HP-ORC & SEAbs)

At fixed operating condition and regardless of the hot source temperature, the values of the turbomachinery optimum parameters barely vary, hence ensuring mitigated off-design performance drops. The higher variation of

the rotational speed is not an issue as a proper design of the gas bearings allows to operate stably on large range of rotor speeds. However, it can be seen that two stages are always required when operating on OP2, as the compressor ratio is too high for only one stage. This explains the reason why the rotor speeds for OP2 are lower than for OP1. Finally, discrepancies exist on the isentropic efficiencies, due to the matching of the turbomachinery's rotational speeds with the range given by Balje's maps. Table 6 presents the turbocompressor design parameters, as well as the ORC and HP evaporation pressures levels for the three HP-ORC working fluids, for the most challenging hot source temperature at 210°C. This table suggests that if R-152a yields the best COP at this specific operating condition, it is also the most challenging regarding rotor speeds, while even though R-245fa offers lower rotor speeds, sub-atmospheric pressures are encountered in the HP loop, which for some manufacturers is prohibitive.

Table 6: Turbocompressor design parameters of the different HP-ORC working fluids at $T_{hot,in}$=210°C

	Fluid	R134a		R245fa		R152a	
Term	OP	OP1	OP2	OP1	OP2	OP1	OP2
Nrot	[krpm]	280	231	157	108	381	314
dt	[mm]	12	13	22	25	11	12
dc,stage1	[mm]	19	20	36	41	18	19
dc,stage2	[mm]	-	19	-	42	-	18
ηis,t (-)	[-]	0.81	0.81	0.81	0.8	0.81	0.81
ηis,c,stage1(-)	[-]	0.86	0.85	0.86	0.84	0.86	0.86
ηis,c,stage2(-)	[-]	-	0.85	-	0.83	-	0.85
Pevap.orc	[bar]	70	70	64	70	21	17
Pevap,hp	[bar]	3.2	1.9	2.8	1.7	0.58	0.3

4.2 Comparison of HP-ORC and SEAbs: thermo-economic trade-off

The thermo-economic optimization of HP-ORC and SEAbs is performed on OP1 and with conditions expressed in Table 1 and Table 4, by using a Multi Objective Optimization (MOO) tool based on a genetic algorithm [35,36]. The output are the Pareto optimum solutions for the two conflicting objectives which are the maximum COP and the minimum investment cost $C_{I,Tot}$. The optimization algorithm expressed as follows:

$$\begin{bmatrix} \max(COP) \\ \min(C_{I,Tot}) \end{bmatrix} = f_{obj}\left(Var\right) \quad (15)$$

where f_{obj} is the objective function including both the thermodynamic and the economic models presented above. Var define the set of thermodynamic cycle variables used for the optimization, whose ranges are presented in Table 7 for the HP-ORC system. The heat exchanger pinches directly influence the performance and the cost, by varying the pressure levels, mass flows and the heat transfer areas. In the HP-ORC, the turbine inlet superheat tends to increase the turbine mechanical power and hence the HP-ORC performance, but at the penalty of ORC evaporator area increase. One integer variable chooses whether the regenerator is present or not in order to identify the conditions where the addition of a regenerator becomes thermo-economically interesting. Finally, the working fluid is also set as an integer variable.

Table 7: Decision variables of the HP-ORC

	#	HP-ORC decision variable		Range
Var :HP-ORC	1	Turbine inlet superheating	DTsh,turb	10-100K
	2	HP-ORC condenser pinch	DTmin,cond	1-20K
	3	HP evaporator pinch	DTmin,evap,hp	1-20K
	4	ORC evaporator pinch	DTmin,evap,orc	1-20K
	5	Presence of regenerator	IsRegen	[0;1]
	6	Working fluid	Fluid	[R-134a;R-152a;R-245fa]

Table 8 presents the thermodynamic decision variables used for the SEAbs cycle. Only the heat exchangers pinch are considered.

Table 8: Decision variables of the SEAbs

	#	SEAbs decision variable		Range
Var :SEAbs	1	SEAbs Generator pinch	DTmin,gen	1-20K
	2	SEAbs Absorber pinch	DTmin,abs	1-20K
	3	SEAbs Condenser pinch	DTmin,cond,ahp	1-20K
	4	SEAbs Evaporator pinch	DTmin,evap,ahp	1-20K

Figure 5a 5b 5c 5d shows the Pareto fronts of both the HP-ORC and SEAbs at the four hot source temperatures (120°C, 150°C, 180°C, 210°C). The two optimizations have been performed with the same number of population and generations ensuring sufficient convergence. For the HP-ORC, the working fluid is a decision variable and is identified by the different symbols and colours on the Pareto front. At 120°C, the Pareto front is determined by the HP-ORC with R-152a for COP below 1.46, and with R-134a above 1.55. In between the SEAbs is the dominating technology. However, the HP-ORC yields the highest COP achievable at 1.66. At 150°C and above, the Pareto front is always dominated by the HP-ORC, first with R-152a, and then with R-134a. The highest HP-ORC's COP is always higher than the SEAbs. Moreover, the higher the hot source temperature is, the smaller the range of feasible SEAbs solutions. As already seen with the operating range comparison, single effect AHPs are not well suited to operate at high hot source temperature due to their limited desorption process with one single generator. To further increase the AHP performance and profit from higher hot source temperatures, the number of effects (stages) has to be increased, linked, however, to the penalty of an increased investment cost, due to the addition of four more heat exchangers with a double effect absorption heat pump. The results therefore suggest that the SEAbs cycle seems to be the more interesting at low hot source temperatures, while the HP-ORC takes over the lead for higher supply temperatures.

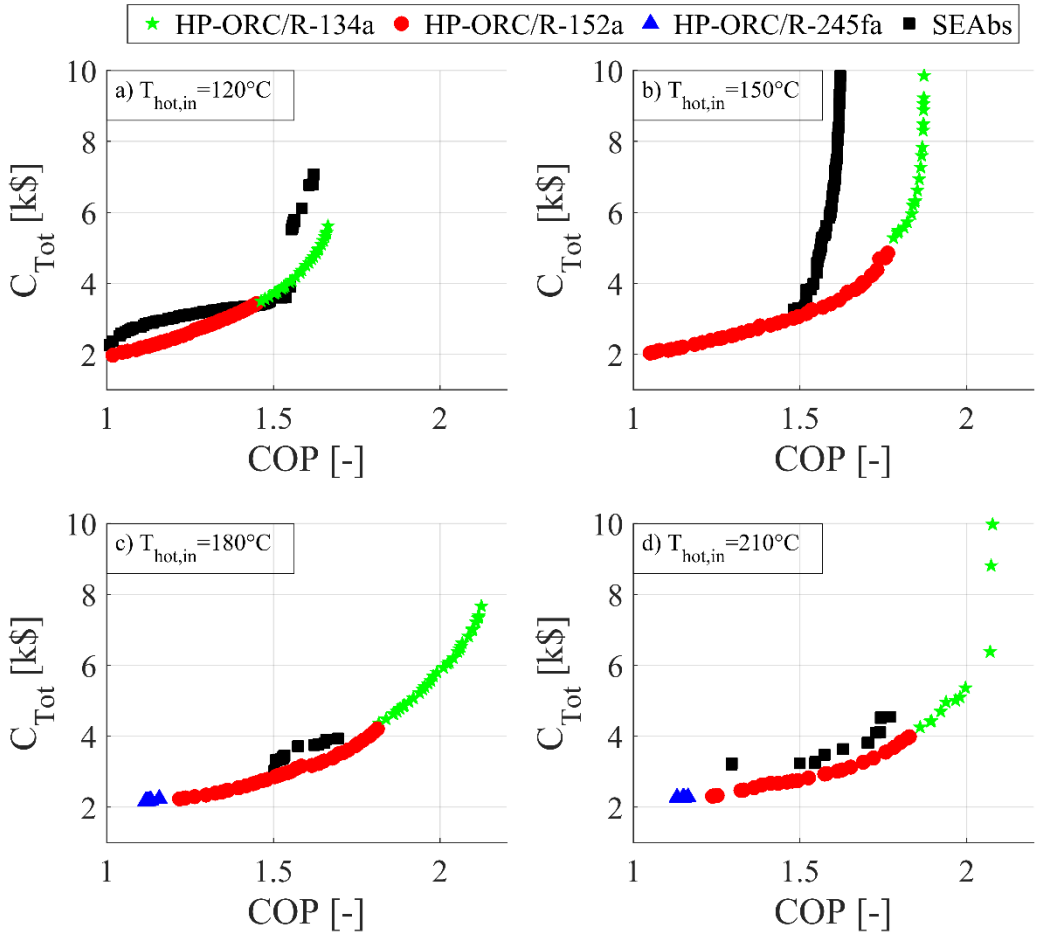


Figure 5 : Thermo-economic optimization of the HP-ORC and SEAbs cycle

4.3 Comparison with existing prototype: potential improvement

A HP-ORC prototype using R134a as working fluid has been developed by Demierre et al [8,11] to serve as a proof of concept for this technology. Table 9 shows a sample of experimental data points including measured temperature levels, rotational speed and heat exchangers areas installed. Note that only one data point is presented here, as it matches at best the boundary conditions chosen for the multi-objective optimization (MOO) of the HP-ORC. For these tests, the hot source temperature inlet is at 180°C, the sink temperature at 35°C and the cold source temperature at 7°C. Two condensers have been tested instead of a single one in order to have more flexibility between the ORC and HP loops. In this prototype, the ORC condenser, the HP condenser and the HP evaporator are PHEs, with heat transfer areas respectively of 2.88 m^2, 1.13 m^2 and 2.88 m^2. The ORC evaporator is composed

of three Double Tube Coils (DTC) in series, with a heat transfer area of 0.23 m^2 each. The cost of the DTC has been assumed through the shell tube cost correlation presented in Table 3.

Table 9: Experimental thermodynamic properties of the HP-ORC proof of concept

Term Unit	Nrot [krpm]	Tevap,hp [°C]	Tcond [°C]	Tevap,orc [°C]	DTsh,turb [K]	DTsc,pump [K]	DTsh,comp [K]	ηis,t [-]	ηis,c [-]	Qsink [kW]
	190	6	32	103	9.9	5	26	0.66	0.69	38

Figure 6 shows the performance of the HP-ORC proof of concept compared with the HP-ORC Pareto resulting from the MOO at a hot source temperature of 180°C. The plot clearly suggests a significant potential for improvement of the current prototype, as it is significantly dominated by the Pareto fronts both in terms of COP and investment cost. The investment cost of the prototype is penalized by having two condensers and three DTCs evaporators instead of one. The use of DTCs instead of PHEs for the ORC evaporator is suboptimal due to their low compactness, as for the same installed volume of heat exchanger, the heat transfer area is lower for DTC. It is observed with the temperatures in the refrigerant side of the ORC evaporator, which are much lower than the hot source temperature (180°C at the thermal oil inlet versus 113°C at the turbine inlet), indicating very high pinch, and hence leading to a significant performance decrease. In a second version of the prototype, the DTCs will be replaced with a properly designed PHE. Furthermore, the measured turbomachinery isentropic efficiencies are lower than the optimal ones given by Balje. This is due to a poor rotor matching, small scale turbomachinery losses not accounted for in Balje's maps, high mass-flow leakage through the CTU [8] or suboptimal CTU design [37]. In a next prototype, an integrally designed and optimized CTU will be implemented, including the detailed design of the turbomachinery, seals, shaft and gas bearings.

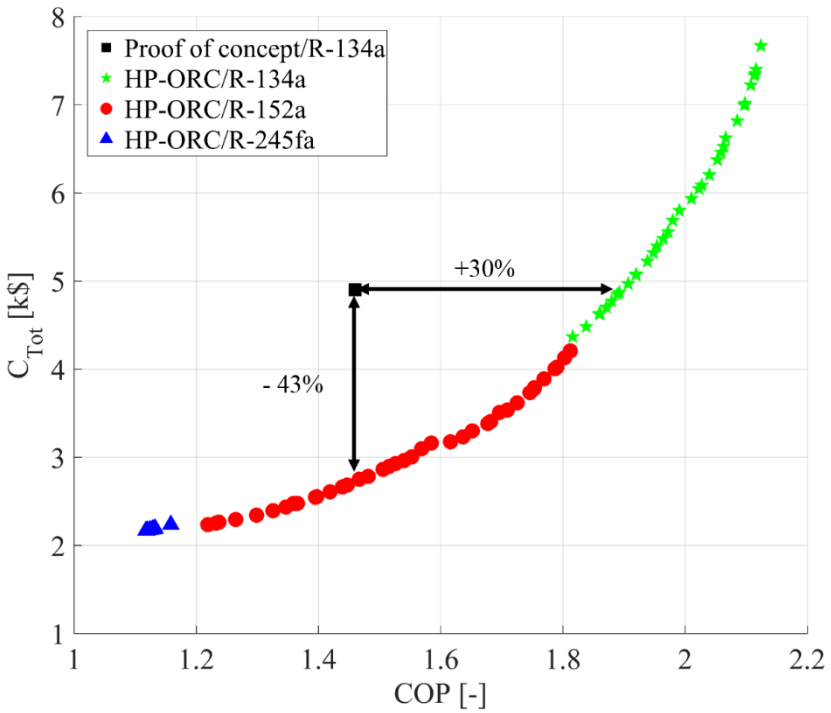


Figure 6 :Comparison of the Pareto front and of the HP-ORC proof of concept

5. Conclusion

An ORC driven Heat Pump (HP-ORC) based on small-scale turbomachinery and a Single Effect Absorption Heat Pump (SEAbs) have been compared for domestic heating application, regarding their performance at different operating conditions and through a thermo-economic optimization. Thorough thermodynamic and economic models of these two systems have been implemented. The economic model is based on the investment cost of the heat exchangers. The thermodynamic model of the HP-ORC includes a reduced order model for predicting the turbomachinery preliminary design and performance. The comparison of the HP-ORC and of the SEAbs on different operating conditions and at one fixed design point show that the two systems are competitive, in particular

at low hot source temperatures. R-134a and R-152a are the best refrigerants for the HP-ORC. Further, the analysis of the turbomachinery's design parameters show the sole performance comparison might be incomplete (rotor speeds, pressure levels...). In a second step, a thermo-economic comparison of the two TDHPs has been performed. The analysis of the Pareto fronts suggest again that the two systems are competitive, with an advantage for the HP-ORC at hot source temperatures above 150°C. In order to increase its performance, more stages or effects should be added to the SEAbs, but at the penalty to increase heat exchangers units, and hence investment cost. The analysis also suggests that a compromise is to be found between R-152a and R-134a working fluids, depending on the COP/Investment cost target of the HP-ORC. Finally, the HP-ORC Pareto front has been compared with the current proof of concept, where a 30% COP improvement or a 43% cost reduction could be achieved. This gap is mainly due to prototype design decision (More HX units for more flexibility), suboptimal ORC evaporator design, suboptimal CTU design and high leakage from the ORC to the HP loop.

6. Acknowledgements

« The authors acknowledge the financial support of the Canton Vaud "100 millions pour les énergies renouvelables et l'efficacité énergétique"

7. Nomenclature

Latin symbols

W	Mechanical Power	W
Q	Heat Rate	W
T	Temperature	K
P	Pressure	Pa
DT_{min}	Minimum approach temperature difference	K
$DT_{sh,turb}$	Turbine superheat	K
$DT_{sh,comp}$	Compressor superheat	K
$DT_{sc,pump}$	Pump subcooling	K
N_{rot}	Rotational speed	rpm
L	PHE width	m
H	PHE height	m
e	Channel spacing	m
A	Area	m^2
C	Cost	$
d	Diameter	m
Var	Decision variables	[-]
Isregen	Regenerator presence	[-]

Greek symbols

η	Efficiency	[-]
β	Chevron angle	rad
Λ	Wavelength of surface corrugation	m

Subscripts and superscripts

Sink	Heat Sink
chill	Cold Source
hot	Hot source
pump	Pump
is	Isentropic
out	Outlet
in	Inlet
regHX	Regenerative Heat Exchangers
t	Turbine
c	Compressor
cond	Condenser/Condensation
evap	Evaporator/Evaporation
Tot	total
I	Investment
stage1,2	Compressor stage
Obj	Objective
Hp	Heat Pump
Orc	ORC
Ahp	Absorption heat pump
Gen	Generator
Abs	Absorber
Precool	Precooler
Shx	Solution heat exchanger

Acronyms

HP- ORC	ORC driven Heat Pump
TDHP	Thermally driven Heat Pump
GEHP	Gas driven Heat Pump
COP	Coefficient of Performance
HP	Heat Pump
ORC	Organic Rankine Cycle
SEAbs	Single Effect Absorption Heat Pump
CTU	Compressor Turbine Unit
AHP	Absorption Heat Pump
HX	Heat Exchanger
GHX	Ground source heat Exchanger
PHE	Plate Heat Exchanger
HC	Helical coil
LMTD	Logarithmic Mean Temperature Difference
LMCD	Logarithmic Mean Concentration Difference

SV	Solution Valve	DTC	Double Tube Coil
MOO	Multi Objective Optimization		

References

[1] Schiffmann J. Small-Scale and Oil-Free Turbocompressor for Refrigeration Applications 2014:1–10.

[2] Schiffmann J, Favrat D. Integrated Design and Optimization of Gas Bearing Supported Rotors. J Mech Des 2010;132:51007. doi:10.1115/1.4001381.

[3] Strong D. Development of a Directly Fired Domestic Heat Pump. University of Oxford, UK, 1980.

[4] Biancardi F, Sitler J, Melikian G. Development and test of solar heating and cooling systems. Int J Refrig 1982;5:351–60.

[5] Prigmore D, Barber R. Cooling with the sun's heat: Design considerations and test data for a Rankine Cycle prototype. Sol Energy 1975;17:185–92.

[6] Wang H, Peterson R, Herron T. Design study of configurations on system COP for a combined ORC (organic Rankine cycle) and VCC (vapor compression cycle). Energy 2011;36:4809–20.

[7] Quoilin S, Broek M Van Den, Declaye S, Dewallef P, Lemort V. Techno-economic survey of organic rankine cycle (ORC) systems. Renew Sustain Energy Rev 2013;22:168–86. doi:10.1016/j.rser.2013.01.028.

[8] Demierre J, Rubino, Antonio, Schiffmann J. Modeling and Experimental Investigation of an Oil-Free Microcompressor-Turbine Unit for an Organic Rankine Cycle Driven Heat Pump. ASME J Eng Gas Turbines Power 2015;137:32602.

[9] Schiffmann J. Enhanced groove geometry for herringbone grooved journal bearings. J Eng Gas Turbines Power 2013;135.

[10] Schiffmann J, Favrat D. The effect of real gas on the properties of herringbone grooved journal bearings. Tribol Int 2010;43:1602–14. doi:10.1016/j.triboint.2010.03.006.

[11] Demierre J, Favrat D, Schiffmann J, Wegele J. Experimental investigation of a Thermally Driven Heat Pump based on a double Organic Rankine Cycle and an oil-free Compressor-Turbine Unit. Int J Refrig 2014;44:91–100.

[12] Mounier V, Mendoza LC, Schiffmann J. Performance Assessment and comparison of Thermally Driven Heat Pump Systems. Int. Congr. Refrig. 2015, Yokahama, Japan: 2015.

[13] Quoilin S, Declaye S, Tchanche BF, Lemort V. Thermo-economic optimization of waste heat recovery Organic Rankine Cycles. Appl Therm Eng 2011;31:2885–93. doi:10.1016/j.applthermaleng.2011.05.014.

[14] Balaras CA, Grossman G, Henning H-M, Infante Ferreira CA, Podesser E, Wang L, et al. Solar air conditioning in Europe—an overview. Renew Sustain Energy Rev 2007;11:299–314. doi:10.1016/j.rser.2005.02.003.

[15] EHPA Testing Regulation. EHPA Testing Regulation Testing of Water / Water and Brine / Water Heat Pumps. 2014.

[16] Bell IH, Wronski J, Quoilin S, Lemort V. Pure and pseudo-pure fluid thermophysical property evaluation and the open-source thermophysical property library coolprop. Ind Eng Chem Res 2014;53:2498–508. doi:10.1021/ie4033999.

[17] Lemmon EW, Huber M., McLinden MO. NIST Standard Reference Database 23: Reference Fluid Thermodynamic and Transport Properties-REFPROP, Version 9.1 2013.

[18] Balje O. Turbomachines - A Guide to Design, Selection, and Theory. John Wiley & Sons; 1980.

[19] Labus J, Bruno C, Coronas A. Review on absorption technology with emphasis on small capacity absorption machines. Therm Sci 2013;17:739–62.

[20] Herold KE, Radermacher R, Klein SA. Absorption Chillers and Heat Pumps, Second Edition. CRC Press; 2016.

[21] Tillner-Roth R, Friend DG. A Helmholtz Free Energy Formulation of the Thermodynamic Properties of the Mixture {Water + Ammonia}. J Phys Chem Ref Data 1998;27:63. doi:10.1063/1.556015.

[22] Conde-Petit M. Thermophysical Properties of NH3 + H2O Mixtures for the Industrial Design of Absorption Refrigeration Equipment. Zurich, Switzerland: 2015.

[23] Kærn MR, Modi A, Jensen JK, Haglind F. An Assessment of Transport Property Estimation Methods for Ammonia–Water Mixtures and Their Influence on Heat Exchanger Size. Int J Thermophys 2015:1–30. doi:10.1007/s10765-015-1857-8.

[24] Henchoz S, Weber C, Maréchal F, Favrat D. Performance and profitability perspectives of a CO2 based district energy network in Geneva's City Centre. Energy 2015;85:221–35. doi:10.1016/j.energy.2015.03.079.

[25] Turton R. Analysis, synthesis and design of chemical processes. Upper Saddle River, N.J.: 2012.

[26] Incropera FP, DeWitt DP, Bergman TL, Lavine AS. Fundamentals of Heat and Mass Transfer. vol. 6th. John Wiley & Sons; 2007. doi:10.1016/j.applthermaleng.2011.03.022.

[27] Lee KB, Chun BH, Lee JC, Lee CH, Kim SH. Experimental analysis of bubble mode in a plate-type absorber. Chem Eng Sci 2002;57:1923–9. doi:10.1016/S0009-2509(02)00089-1.

[28] Amalfi RL, Vakili-Farahani F, Thome JR. Flow boiling and frictional pressure gradients in plate heat exchangers: part 1, review and experimental database. Int J Refrig 2015. doi:10.1016/j.ijrefrig.2015.07.010.

[29] Martin H. A theoretical approach to predict the performance of chevron-type plate heat exchangers. Chem Eng Process Process Intensif 1996;35:301–10. doi:10.1016/0255-2701(95)04129-X.

[30] Yan YY, Lio HC, Lin TF. Condensation heat transfer and pressure drop of refrigerant R134a in a plate heat exchanger. Int J Heat Mass Transf 1999;42:993–1006.

[31] Danilova GN, Azarrskov VM, Zemskov BB. Teploobmen v plastinchatihispariteljan razichnole geometri (Heat transfer in plate evaporators of different geometry). Kholod Tek 1981;4:25–31.

[32] Táboas F, Vallès M, Bourouis M, Coronas A. Assessment of boiling heat transfer and pressure drop correlations of ammonia/water mixture in a plate heat exchanger. Int J Refrig 2012;35:633–44. doi:10.1016/j.ijrefrig.2011.10.003.

[33] Qaswari AM., Treece RJ, Blakeley RE. The Design and Development of an Absorption Cycle Heat Pump Optimised for the Achievement of Maximum Coefficient of Performance. Luxembourg: COMMISSION OF THE EUROPEAN COMMUNITIES; 1972.

[34] palmstiernas. FLOW REGULATOR TYPE RW-15 AISI 316L 2016.

[35] Molyneaux A, Leyland G, Favrat D. Environomic multi-objective optimisation of a district heating network considering centralized and decentralized heat pumps. Energy 2010;35:751–8. doi:10.1016/j.energy.2009.09.028.

[36] Leyland G. Multi-Objective optimization applied to industrial energy problems, Ph.D thesis. Ecole Polytechnique Fédérale de Lausanne EPFL, 2002.

[37] Schiffmann J. Integrated Design and Multi-Objective Optimization of a Single Stage Heat-Pump Turbocompressor. J Turbomach 2015;137. doi:10.1115/1.4029123.